Interatomic electronic decay following multiple ionization of rare gas dimers

Inner-valence vacancy states in molecules are usually not subject to autoionization and thus relax via fluorescence decay and/or dissociation. In 1997, Cederbaum *et al*. noted that such inner-valence vacancy states may be subject to autoionization if they are in close proximity to other molecules. They called this new type of autoionization intermolecular or interatomic Coulombic decay (ICD) [1]. In ICD, two electrons are involved: one electron fills the vacancy and another electron is emitted as an ICD electron. If the electron that fills the vacancy originally belongs to the species with the vacancy and the electron that is emitted originally belongs to the other neighboring species, the process is called direct ICD (Fig. 1(a)). If the emitted electron originally belongs to the species with the vacancy and the electron that fills the vacancy originally belongs to the other neighboring species, the process is called exchange ICD (Fig. 1(b)). Exchange ICD is usually much weaker than direct ICD but becomes experimentally visible if direct ICD is energetically closed. If both electrons that participate in the decay originally belong to the neighboring species that does not have the vacancy, the process is called electron-transfer mediated decay (ETMD) (Fig. 1(c)). ETMD is usually much weaker than ICD but may become visible if ICD is energetically closed. If an inner-valence double-vacancy state is created, another class of ICD may occur, i.e., three-electron ICD, in which two outer-valence electrons fill two inner-valence vacancies and another electron is emitted from outer-valence orbitals. Three-electron ICD is usually much weaker than two-electron ICD but may become visible if two-electron ICD is energetically closed.

We have investigated the above-described different interatomic electronic decay processes in the rare gas dimers NeAr and Ar_2, as typical prototype examples, by electron-ion-ion coincidence momentum-imaging at beamline **BL27SU**. The coincidence momentum-imaging is based on recording the electron and ion times-of-flight (TOFs) with position- and time-sensitive multihit-capable detectors. Knowledge of position and arrival time on the particle detectors, (*x,y,t*), allows us to extract information about the 3D momentum of each particle. The electron and ion TOF spectrometers were placed face to face. The TOF spectrometer axis was horizontal and perpendicular to both the horizontal photon beam and the vertical cluster beam. The argon dimers (Ar_2) were produced by the expansion of argon gas at 300 K, while the heterodimers (NeAr) were produced by expanding a mixture of neon and argon gases at 103 K. Signals from Ar_2 and NeAr were extracted by momentum conservation for ion pair formation.

For NeAr, when we tuned the photon energy above the Ne 1s ionization threshold, we found a significant amount of Ne^{2+}-Ar^{+} ion-pair formation. Figure 2(a) depicts kinetic energy release (KER), i.e., the sum of the kinetic energies for the two dissociating ions Ne^{2+} and Ar^{+} recorded in coincidence. Assuming the Coulomb repulsion between Ne^{2+} and Ar^{+}, we found that the measured KER peak of ~8 eV corresponds to an internuclear distance of 3.5 Å, in good agreement with the equilibrium distance of the neutral ground state of NeAr. Figure 2(b) depicts the energy distribution of electrons recorded in coincidence with

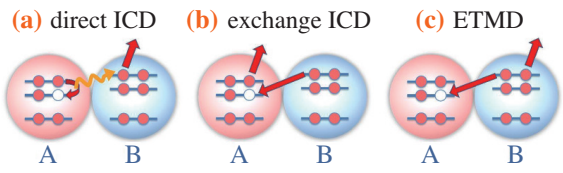

Fig. 1. Schematic diagrams of **(a)** direct ICD, **(b)** exchange ICD, and **(c)** ETMD. [4]

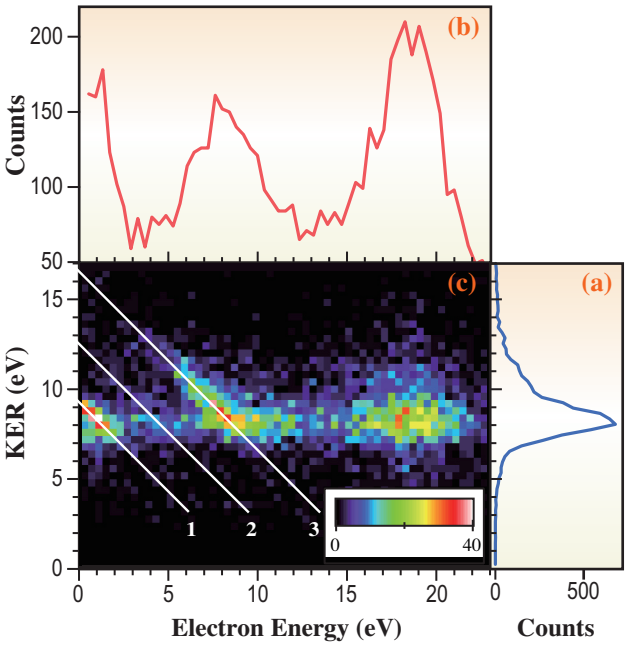

Fig. 2. **(a)** KER for Ne^{2+}-Ar^{+} fragmentation channel. **(b)** Kinetic energy distribution of electrons detected in coincidence with Ne^{2+}-Ar^{+} pairs. **(c)** Correlation map between electron emission and KER. The three straight lines of slope –1 correspond to the energies of the ICD transitions. [2]

Ne^{2+}-Ar^{+} ion pairs. The peak that appears at ~19 eV corresponds to the Ne 1*s* photoelectron peak, while other peaks at low energies correspond to the ICD electron emission. Figure 2(c) shows a correlation between the electron emission and the KER recorded in coincidence. In this correlation diagram, the island of the ICD transition appears as the line of slope –1, because the sum of ICD electron kinetic energy and KER is constant in the ICD transition. The three lines with slope –1 correspond to the sum energies of the expected direct ICD transitions: (1) $Ne^{2+}(2s^{-1}2p^{-1}\ ^3P)Ar$ to $Ne^{2+}(2p^{-2}\ ^3P)$-$Ar^{+}(3p^{-1}\ ^2P)$, (2) $Ne^{2+}\ (2s^{-1}2p^{-1}\ ^1P)Ar$ to $Ne^{2+}(2p^{-2}\ ^1S)$-$Ar^{+}(3p^{-1}\ ^2P)$, and (3) $Ne^{2+}(2s^{-1}2p^{-1}\ ^1P)Ar$ to $Ne^{2+}(2p^{-2}\ ^1D)$-$Ar^{+}(3p^{-1}\ ^2P)$. In the figure, we can identify all three ICD transitions [2]. We cannot identify any exchange ICD or ETMD here.

When we tuned the photon energy above the Ar 2*p* ionization threshold, we found a significant amount of Ne^{+}-Ar^{2+} ion-pair formation. Detecting two electrons with the Ne^{+}-Ar^{2+} ion pair in coincidence (i.e., four-fold coincidence), we confirmed that the low-energy electrons below 2 eV are emitted following Ar 2*p* Auger decay after 2*p* photoionization, resulting in the ionization of the neighboring Ne atom. Thus, this low energy electron emission may be assigned as ICD. Figure 3(b) depicts the distribution of KER for Ne^{+} and Ar^{2+}, whereas Fig. 3(c) shows a schematic energy diagram for the initial and final states of ICD. Assignments of these initial and final states are given in the figure caption. The *x*-axis is given by the inverse of the internuclear distance (1/R decreases to the right); thus, we can directly correlate the value of 1/R to KER in Fig. 3(b). From this energy scheme, we expect four transitions to contribute to the KER spectrum: from A to 1, from B to 1, from C to 1, and from D to 1. The transition from B to 1 peaking at 9.4 eV is three-electron exchange ICD. The reasonable agreement of simulated KER spectra given in Fig. 3(a) to the experimental one in Fig. 3(b) supports this assignment. This is the first observation of three-electron ICD [3]. Although three-electron ICD relies on higher-order correlations, it became visible because lower-order ICD is energetically closed for the state B.

For Ar_2, we focus on triple ionization that forms Ar^{3+}-Ar as initial states of ICD and ETMD. The Ar^{3+}-Ar^{+} ion pair is expected to be produced by ICD, and Ar^{2+}-Ar^{2+} ion pair formation implies that ETMD occurs. By detecting low-energy electrons in coincidence with Ar^{3+}-Ar^{+} and Ar^{2+}-Ar^{2+} (i.e., three-fold coincidence) we could identify the ICD and ETMD processes, respectively. This is the first observation of ETMD [4]. ETMD became visible because, for low-lying Ar^{3+}-Ar inner-valence-hole states, ICD is energetically closed, while ETMD is open.

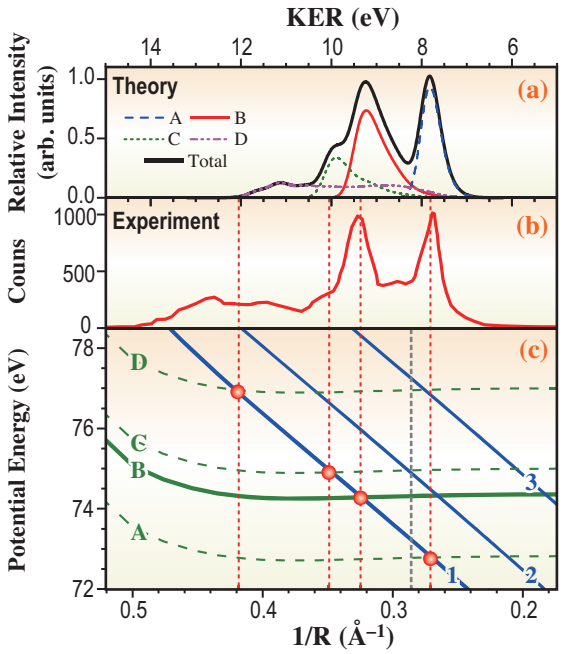

Fig. 3. **(a)** Simulated partial and total KER distributions for the transitions from the initial states A–D. **(b)** Experimental total KER distribution. **(c)** Schematic energy diagram for the initial (labeled A-D) and final (labeled 1-3) states of the ICDs. A, $Ne\text{-}Ar^{2+}(3p^{-3}(^2P)3d\ ^1P)$; B, $Ne\text{-}Ar^{2+}(3s^{-2}\ ^1S)$; C, $Ne\text{-}Ar^{2+}(3p^{-3}(^2P)4p\ ^1S)$; D, $Ne\text{-}Ar^{2+}(3p^{-3}(^2P)4d\ ^1P,^3D,^3P)$. 1, $Ne^{+}(2p^{-1}\ ^2P)$-$Ar^{2+}(3p^{-2}\ ^3P)$; 2, $Ne^{+}(2p^{-1}\ ^2P)$-$Ar^{2+}(3p^{-2}\ ^1D)$; 3, $Ne^{+}(2p^{-1}\ ^2P)$-$Ar^{2+}(3p^{-2}\ ^1S)$. [3]

Kiyoshi Ueda*, Kentaro Sakai and Hironobu Fukuzawa

Institute of Multidisciplinary Research
for Advanced Materials, Tohoku University

*E-mail: ueda@tagen.tohoku.ac.jp

References

[1] L.S. Cederbaum *et al.*: Phys. Rev. Lett. **79** (1997) 4778.
[2] *T. Ouchi, K. Sakai, H. Fukuzawa, I. Higuchi, Ph.V. Demekhin, Y.-C. Chiang, S.D. Stoychev, A.I. Kuleff, T. Mazza, M. Schöffler, K. Nagaya, M. Yao, Y. Tamenori, N. Saito and K. Ueda: Phys. Rev. A* ***83*** *(2011) 053415.*
[3] *T. Ouchi, K. Sakai, H. Fukuzawa, X.-J. Liu, I. Higuchi, Y. Tamenori, K. Nagaya, H. Iwayama, M. Yao, D. Zhang, D. Ding, A.I. Kuleff, S.D. Stoychev, Ph.V. Demekhin, N. Saito and K. Ueda: Phys. Rev. Lett.* ***107*** *(2011) 053401.*
[4] *K. Sakai, S. Stoychev, T. Ouchi, I. Higuchi, M. Schöffler, T. Mazza, H. Fukuzawa, K. Nagaya, M. Yao, Y. Tamenori, A.I. Kuleff, N. Saito and K. Ueda: Phys. Rev. Lett.* ***106*** *(2011) 033401.*